

Cyclocondensation of Anthranilamide with Aldehydes on Gallium-Containing MCM-22 Zeolite Materials

Preeti Sahu, Adarsh Sahu,* and Ayyamperumal Sakthivel*

Cite This: *ACS Omega* 2021, 6, 28828–28837

Read Online

ACCESS |



Metrics & More

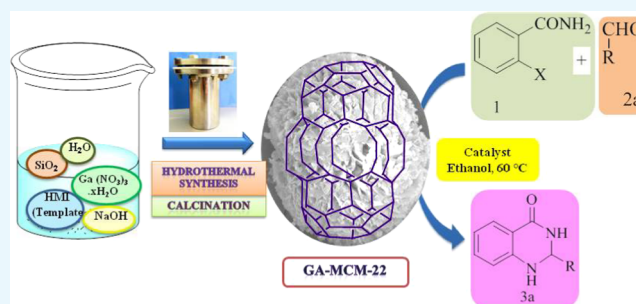


Article Recommendations



Supporting Information

ABSTRACT: A gallium-containing MCM-22 (Mobil Composition of Matter No. 22) zeolite material was prepared using a simple hydrothermal method. Fourier transform infrared spectroscopy analysis and powder X-ray diffraction provide evidence of the formation of a pure MCM-22 phase framework and an MWW (MCM-tWenty-tWo) structure. Scanning electron microscopy images showed a uniform spherical shape, interpenetrating the platelet structure and a uniform particle size of approximately 6 μm . ^{71}Ga nuclear magnetic resonance studies confirmed the presence of gallium in both the tetrahedral framework and the octahedral extra-framework environment. From the sorption studies, the presence of strong acidic sites and the microporous nature of the material were evident. The resultant Ga-MCM-22 material showed an excellent isolated yield of 95% in the synthesis of 2,3-dihydroquinazolin-4(1H)-ones by cyclocondensation of anthranilamide with aldehydes in ethanol. The scope of the reaction was further explored by employing various cyclic, aromatic, and aliphatic aldehydes with anthranilamide. The results provide a very good yield (85–95%). A significant advantage of the developed protocol includes high yield, use of a green solvent, and easy removal of the catalyst through filtration within a short reaction time.



1. INTRODUCTION

Zeolites are well-defined microporous aluminosilicate materials with high crystallinity, which possess extensive applications as heterogeneous catalysts in petrochemical industries and refineries. A wide range of their applications is reported in the fine chemical industry, petroleum-petrochemical, pharmaceutical, and cosmetic industries owing to their tunable pore size and acid–base properties.^{1–8} Among the 240 zeolites recognized by the International Zeolite Association, the MCM-22 zeolite is one of the interesting zeolites, currently receiving significant attention in commercial applications due to its unique features, such as external pocket, thermal stability, large surface area, and adsorption capacity. Mobil Oil Co. researchers developed a crystalline porous material with the MWW (MCM-tWenty-tWo) topology in 1991.⁶ Two independent pore systems form the internal structure of this medium pore opening-layered zeolite. The MCM-22 framework combined 10 membered rings (MRs) (4 Å × 5.9 Å), a two-dimensional interlayer sinusoidal channel, and 12 MR supercages (7.1 Å × 7.1 Å × 18.2 Å) connected by 10 MR apertures. An interesting feature of these deemed “cups” (supercages) is that half of them are present on the external surface of the crystals, and these cups are rich in acid sites available for large molecule transformations. MCM-22-based materials are explored as potential catalysts for various organic transformations, namely, selective aromatic alkylation, isomerization, and disproportionation. They also have potential for the transformation of paraffin to aromatics and olefins.^{9–19}

The acidic sites and the strength of acidic sites on the zeolite framework can be tuned by introducing heteroatoms, which can transform its physicochemical properties and catalytic activity. The introduction of trivalent gallium into the framework of zeolite facilitates remarkable physicochemical and catalytic properties. The presence of trivalent gallium in the framework and nonframework zeolitic sites provides abundant surface medium-strong acid sites.^{20–27} The presence of heteroatoms in the extra-framework species and tetrahedral framework sites provides bifunctional active sites.^{20–27} In the MCM-22 case, isomorphous substitution other than trivalent aluminum species is interesting in tuning the physicochemical properties. Few reports are available on the gallium-exchanged MCM-22 zeolite. For example, Kumar et al. described Ga-MCM-22 zeolite synthesis, characterization, and its application for the aromatization of *n*-butane. Wang et al. explored propane dehydrogenation. The term gallosilicates refers to the absence of Al species although it is permissible to use the seeds for syntheses.²⁴ Morrison and Rubin developed gallosilicate MCM-22, which showed high selectivity for toluene in

Received: July 14, 2021

Accepted: September 23, 2021

Published: October 20, 2021



methylcyclohexane hydrogenation.^{28,29} Later, Kim et al. reported the synthesis and characterization of gallium containing MCM-22. Similarly, Fehete et al. studied the physicochemical properties of synthesized Ga-MCM-22 and examined it for toluene disproportionation.^{19,23,24,27–29} Gallium raised interest in isomorphous substitution during 1990, where UPO-BP introduced gallium in a pentasil catalyst, that is to say, ZSM-5 (Zeolite Socony Mobil-5) in a cycle process as a catalyst for producing aromatic compounds from short-chain hydrocarbons. Gallium-modified zeolites have achieved remarkable success in various catalytic processes. Some of them are biomass copyrolysis and dehydrogenation.^{20,24,30} The application of zeolites as catalysts for fine chemical production is explored at a limited level. In this regard, this study reports that 2,3-dihydroquinazolin-4(1H)-ones are an important class of heterocyclic compounds, which has been applied in agrochemicals³¹ and medicinal³² and organic chemistry.³³ Consequently, the central structural motifs of biological interest coupled with another heterocyclic ring have exhibited therapeutic potential in different domains such as antileishmanial,³⁴ anticancer,³⁵ antimicrobial,³⁶ and antituberculosis.³⁷ Numerous methods have been reported for the synthesis of 2,3-dihydroquinazolin-4(1H)-ones, which include the multicomponent reaction of isatoic anhydride, ammonium chloride, and aldehydes using indium chloride,³⁸ condensation of 2-aminobenzamide with aldehydes using zirconium(IV) chloride (2 mol(M)%) in ethanol,³⁹ and palladium-catalyzed cyclocarbonylation of *o*-iodoanilines.⁴⁰ Some of the reported methodologies produce good results. However, these reactions are limited because of their long reaction time, expensive catalyst, harsh reaction conditions, low yield of the product, and tedious workup conditions. Thus, it is crucial to develop simple, efficient, eco-friendly, inexpensive, and easy workup methodologies for the synthesis of 2,3-dihydroquinazolin-4(1H)-ones.

This study focuses on the synthesis of gallium that contains MCM-22 and investigates its cyclocondensation reaction of anthranilamide with aldehydes in ethanol. The goal is to report the efficient, quick, inexpensive, low catalyst loading, eco-friendly, greener synthesis of 2,3-dihydroquinazolin-4(1H)-ones. An important utility of the reaction is the ability of the compound to be isolated by filtration.

2. EXPERIMENTAL SECTION

2.1. Synthesis. The Ga-MCM-22 material was synthesized using an appropriate molar gel ratio of SiO₂:0.3 NaOH:0.6 HMI:*x* Ga₂O₃:*y* H₂O. Different synthetic conditions were applied for the synthesis by varying the concentrations of *x* and *y*, which is summarized in Table 1. For the synthesis of the catalysts, two steps are involved. The first step involves the

synthesis of a mixture of NaOH (sodium hydroxide, Sisco Research Laboratories, SRL, India) solution (in Millipore water) and colloidal silica (SiO₂, Sigma-Aldrich, LUDOX HS-40, 40 wt %) under continuous stirring followed by the addition of gallium nitrate (Ga(NO₃)₃ · *x*H₂O, Alfa Aesar, 99.9% metal basis) solution. The prepared gel was transferred to a stainless steel Teflon-lined autoclave and kept in a preheated (180 °C) oven for aging. Furthermore, the solution was cooled down and mixed with hexamethyleneimine (HMI, Alfa Aesar) and NaOH solution. Thereafter, the solution was transferred to the stainless steel Teflon-lined autoclave for 168 h and kept in a preheated oven at 155 °C. Furthermore, the prepared gel was cooled down to room temperature, filtered, washed with Millipore water, and dried at 80 °C overnight. Then the sample was calcined at 550 °C for 6 h under an air flow of 50–100 mL/min.^{41,42} The calcined sample was ion-exchanged with a 1 M solution of ammonium acetate to obtain protons from the catalyst. All the reagents used in the synthesis were purchased from commercial sources and used without further purification.

2.2. Characterization. The nature of the structural framework and structural building unit was analyzed by Fourier transform infrared (FTIR) spectroscopy in the range of 400–4000 cm⁻¹ with a PerkinElmer Spectrum using the KBr pellet technique. The powder X-ray diffraction (XRD) pattern was collected using a Rigaku MiniFlex 600 diffractometer with nickel-filtered Cu K α radiation. Diffractograms were recorded in a 2 θ range from 5 to 45° with a step size of 0.02° and a scan rate of 2°/min. The morphology and size of the zeolites were characterized using an FEI Nova NanoSEM 450 scanning electron microscope operated at 5.00 kV. Thermogravimetric analysis (TGA) was performed using a PerkinElmer STA-6000 from room temperature up to 700 °C at a rate of 10 °C/min under a nitrogen environment. The Brunauer–Emmett–Teller (BET) surface area and N₂ adsorption–desorption of the calcined samples were determined by Quantachrome Instruments Autosorb-IQ volumetric adsorption analyzer. The samples were degassed at –200 °C. The BET and *t*-plot micropore surface areas were calculated in a relative pressure (*p/p*₀) range of 0–0.1 over the adsorption branch of the isotherm. The Barrett–Joyner–Halenda (BJH) pore size distribution was obtained from the desorption branch of the isotherm. Other textural properties like pore volume were determined from the isotherm data. The acidity measurement was carried out using a BELCAT-M (Japan) temperature-programmed desorption (TPD) instrument equipped with a thermal conductivity detector. The sample was preheated in a quartz reactor at 500 °C for 30 min in a He flow. Ammonia was adsorbed at 100 °C for 30 min. Ammonia desorption was carried out at 100 °C for 15 min to remove any physisorbed ammonia. TPD of ammonia was performed from 50 to 700 °C at a heating rate 10 °C/min and a helium flow of 30 mL/min. The solid-state nuclear magnetic resonance (NMR) experiments were performed on a Bruker Avance III HD 400 MHz MAS spectrometer equipped with a 4 mm CP/MAS probe (high-resolution solid-state apparatus) and a superconducting magnet with a field of 9.4 T. The samples were recorded at a particular frequency packed in 4 mm zirconia rotors at a spinning speed of 7 kHz. The ²⁹Si NMR spectra were recorded at 79.5 MHz with a pulse duration of 3.5 μ s with a delay of 10 s and 10 scans. The ⁷¹Ga NMR spectra were recorded at 122 MHz with a pulse duration of 3.5 μ s with a delay of 1 s and 7150 scans.

Table 1. Molar Composition and Synthetic Conditions of the Synthesized Catalysts

sample no.	gel ratio				final gel temperature (K)	final gel duration (H)
	Si/Ga	Na/Si	HMI/Si	H ₂ O/Si		
Ga-MCM-22 (A)	20	0.3	0.6	45	428	240
Ga-MCM-22 (B)	30	0.3	0.6	45	428	240
Ga-MCM-22 (C)	30	0.3	0.6	45	428	168

^1H NMR and ^{13}C NMR experiments were conducted using a Bruker DX 500 MHz. The chemical shift was reported in parts per million relative to tetramethylsilane as an internal standard. The ^1H NMR spectra were referenced with respect to the residual deuterated chloroform (CDCl_3) and dimethyl sulfoxide or $\text{DMSO-}d_6$ at 7.29 and 3.34 and 2.51 ppm. The coupling constants were reported in hertz (Hz). The ^{13}C NMR spectrum pattern was fully decoupled and was referenced to the middle peak of the solvent at 77 (CDCl_3) and 40 ppm ($\text{DMSO-}d_6$). Splitting patterns were denoted as s, singlet; d, doublet; dd, doublet of doublet; and m, multiplet. The infrared spectrum of the reaction product was recorded using an FTIR-8400S (Shimadzu). Compounds were routinely analyzed for their purity on a silica gel GF254 visualized under ultraviolet (UV) light at a wavelength of 254 nm.

2.3. Catalytic Study. The cyclocondensation reaction was carried out in a two-neck round-bottom (RB) flask equipped with a condenser. Normally, an activated catalyst (preheated at 120 °C for 30 min) was added to ethanol in the RB flask with continuous stirring and refluxed in an oil bath. After 5 min of a typical run, 1 mM anthranilamide was added followed by the addition of aldehyde under stirring conditions. The progress of the reaction was monitored by thin-layer chromatography (TLC). After completion, the reaction product was isolated by simply separating the catalyst by filtration followed by purification of the compound using columns. Ethanol was dried under a reduced pressure to obtain an analytically pure quinazolin-4(3H)-one derivative. The obtained compound was characterized using melting point and NMR spectroscopy without further purification.

2.3.1. ^1H and ^{13}C NMR Spectra of the Synthesized Compounds. **2.3.1.1. 2-phenyl-2,3-dihydroquinazolin-4(1H)-one (1).** Yield: 95% (white solid) mp 219–2 °C. ^1H NMR (400 MHz, CDCl_3) (ppm): 8.05 (s, 1H), 7.95 (d, $J = 5$ Hz, 1H), 7.60–7.56 (m, 1H), 7.44 (t, $J = 5$ Hz, 2H), 7.33 (t, $J = 10$ Hz, 1H), 6.90 (t, 1H), 6.6 (s, 3H); ^{13}C NMR (100 MHz, CDCl_3): 164, 147, 138, 134, 130, 128, 126, 119, 114, 99, 69.

2.3.1.2. 2-(4-hydroxyphenyl)quinazolin-4(3H)-one. ^1H NMR (500 MHz, CDCl_3) (ppm): 8.08 (s, 1H), 7.94 (d, $J = 8$ Hz, 1H), 7.59–7.56 (m, 1H), 7.45 (t, $J = 8$ Hz, 1H), 7.34 (t, $J = 8$ Hz, 1H), 7.23 (t, 1H), 6.90 (s, 1H), 6.68–6.66 (m, 1H), 6.00 (s, 1H), 5.90 (s, 1H).

2.3.1.3. 2-(4-(diethylamino)phenyl)-2,3-dihydroquinazolin-4(1H)-one. ^1H NMR (500 MHz, CDCl_3) (ppm): 8.09 (s, 1H), 7.39 (d, $J = 8$ Hz, 1H), 7.32 (d, $J = 8$ Hz, 1H), 7.20 (d, $J = 8$ Hz, 2H), 7.04 (m, 2H), 4.93 (s, 1H), 1.69–1.53 (m, 4H), 1.31–1.11 (m, 6H).

2.3.1.4. 2-(*p*-tolyl)-2,3-dihydroquinazolin-4(1H)-one. ^1H NMR (500 MHz, CDCl_3) (ppm): 8.04 (d, $J = 8$ Hz, 1H), 7.94 (t, $J = 8$ Hz, 2H), 7.44 (q, $J = 8$ Hz, 2H), 7.39 (t, $J = 8$ Hz, 1H), 6.90 (t, $J = 8$ Hz, 1H), 6.66 (d, $J = 8$ Hz, 1H), 6.00 (s, 1H), 5.90 (s, 1H), 5.83 (s, 1H).

2.3.1.5. 2-(4-chlorophenyl)-2,3-dihydroquinazolin-4(1H)-one. ^1H NMR (500 MHz, CDCl_3) (ppm): 8.04 (d, $J = 8$ Hz, 1H), 7.93 (d, $J = 8$ Hz, 1H), 7.80 (s, 1H), 7.53 (d, $J = 8$ Hz, 1H), 7.40 (d, $J = 8$ Hz, 2H), 7.34 (t, $J = 6$ Hz, 1H), 6.91 (t, $J = 8$ Hz, 1H), 6.66 (d, $J = 6$ Hz, 1H), 5.88 (s, 1H), 5.83 (s, 1H).

2.3.1.6. 2-(1-hydroxycyclohexyl)-2,3-dihydroquinazolin-4(1H)-one. ^1H NMR (400 MHz, $\text{DMSO-}d_6$) (ppm): 8.36 (s, 1H), 7.62 (d, $J = 8$ Hz, 3H), 7.80 (d, $J = 8$ Hz, 2H), 4.93 (s, 2H), 1.90–1.86 (m, 2H), 1.72 (t, $J = 8$ Hz, 3H), 1.64 (t, $J = 10$ Hz, 1H), 1.48 (s, 1H), 1.40 (s, 1H), 1.26 (d, $J = 10$ Hz, 1H).

3. RESULTS AND DISCUSSION

As summarized in Table 1, the Ga-MCM-22 samples were prepared with different synthetic conditions. Among the

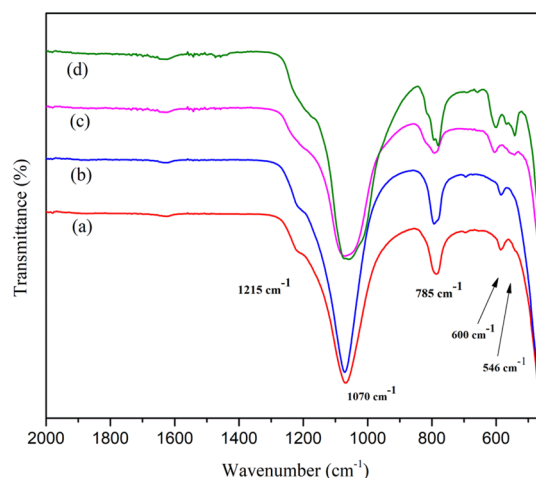


Figure 1. FTIR spectra of calcined samples (a) Ga-MCM-22 (A), (b) Ga-MCM-22 (B), (c) Ga-MCM-22 (C) as-synthesized, and (d) calcined Ga-MCM-22 (C).

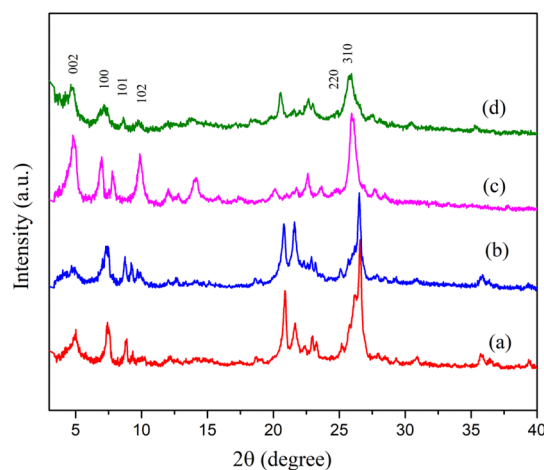


Figure 2. XRD patterns of calcined samples (a) Ga-MCM-22 (A), (b) Ga-MCM-22 (B), (c) Ga-MCM-22 (C) as-synthesized, and (d) calcined Ga-MCM-22 (C).

several batches of samples prepared, the sample derived with a Si/Ga ratio of 30 and an $\text{H}_2\text{O}/\text{Si}$ ratio of 20 in 168 h at 428 K (Ga-MCM-22 (C)) showed characteristic doublet framework vibration and better crystallinity in the powder XRD spectra (Figures 1 and 2). Ga-MCM-22 (c) sample were used for the further characterization and study catalytic cyclocondensation of anthranilamide with aldehydes.

Figure 1 shows the FTIR spectra of as-synthesized, calcined aluminum, and gallium-containing MCM-22 samples. The vibrational bands at 1245 and 1080 cm^{-1} are related to external and internal linkages of Si-O-Si (asymmetric stretching). The band at 790 cm^{-1} is related to the Si-O-Si tetrahedral external linkage (symmetric stretching). The doublet between 600 and 500 cm^{-1} is related to external linkages as secondary building units (double six-membered ring or D6R), referred to as a structural band of MWW characteristics. The band at 445 cm^{-1} is related to internal tetrahedral (T-O bend) framework sites. The FTIR spectra of as-synthesized and calcined Ga-

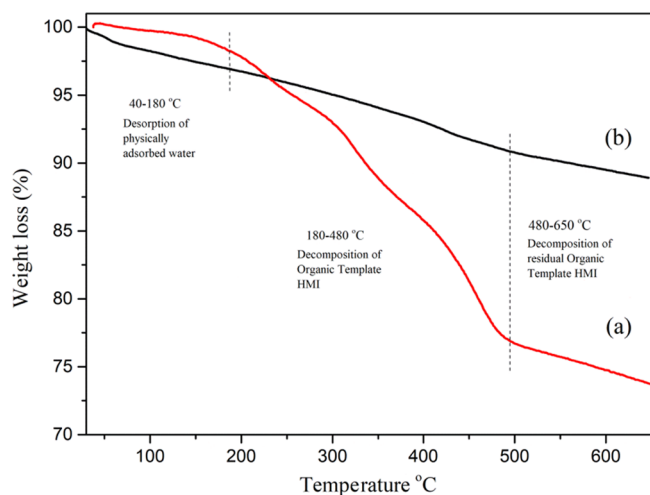


Figure 3. TGA thermogram of (a) MCM-22 and (b) Ga-MCM-22.

MCM-22 showed all the vibrational bands similar to parent Al-MCM-22 as reported in the literature.⁴³ However, a vibrational band shifted from 549 to 551 cm^{-1} and 599 to 605 cm^{-1} . A shift was also observed for the framework vibrational bands that appeared around 1018 and 1071 cm^{-1} , at a lower frequency for Ga-MCM-22, which may be due to the presence

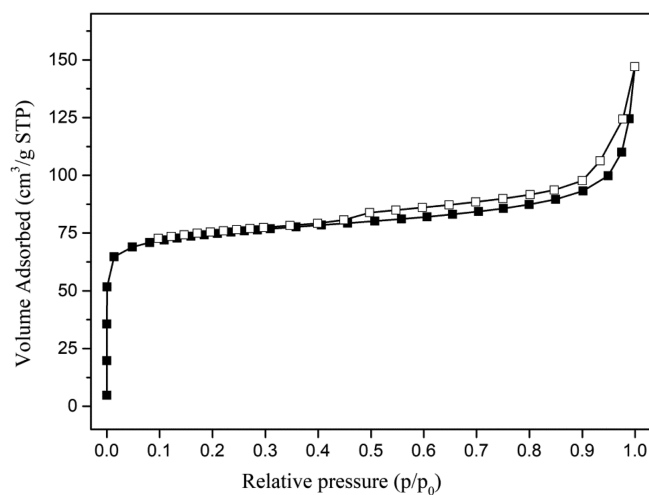


Figure 5. Nitrogen adsorption isotherm of the Ga-MCM-22 sample.

Table 2. Textural Properties of MCM-22 and Ga-MCM-22

s. no.	sample	surface area (m^2/g)		pore volume (cm^3/g)	
		BET	micropore	BJH	
1	commercial-MCM-22	487	0.20	0.36	
2	Ga-MCM-22 (30)	263	0.197	0.095	

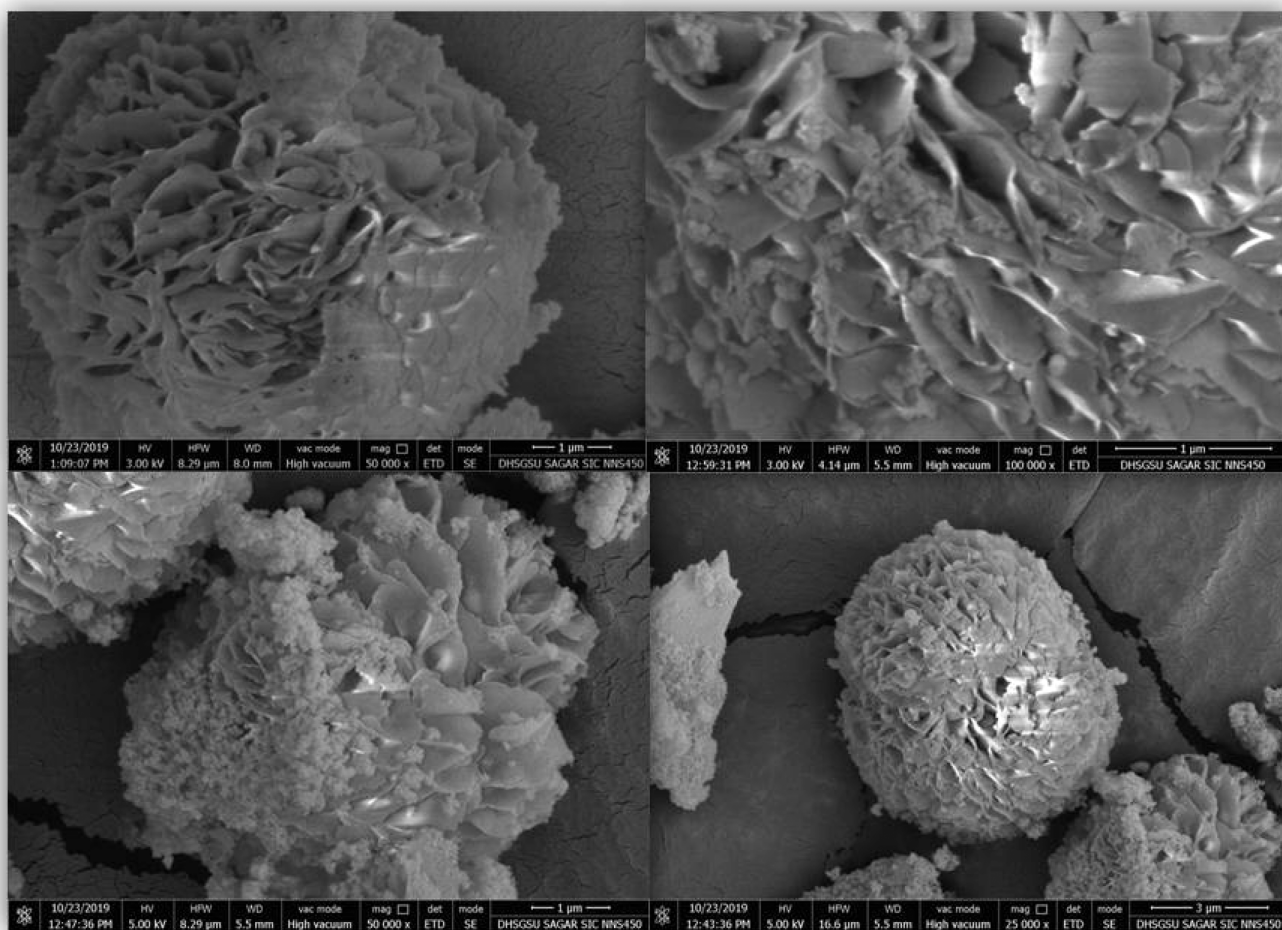


Figure 4. Scanning electron microscopy (SEM) images of the Ga-MCM-22 sample.

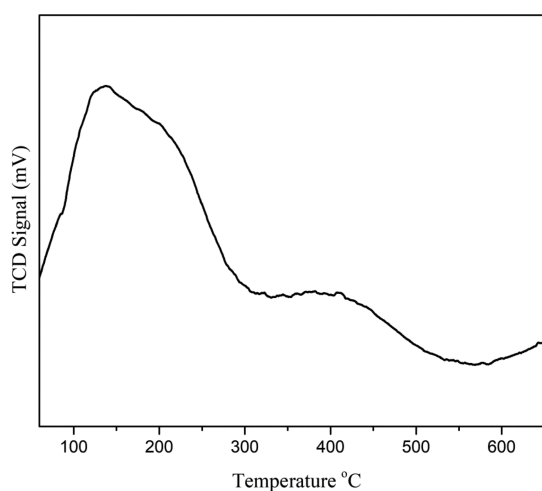


Figure 6. Ammonia TPD curve of the Ga-MCM-22 sample.

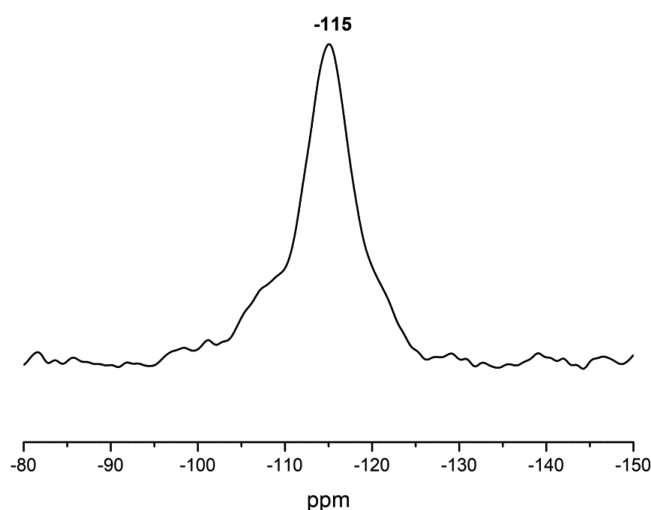


Figure 7. ^{29}Si NMR spectrum of the calcined Ga-MCM-22 sample.

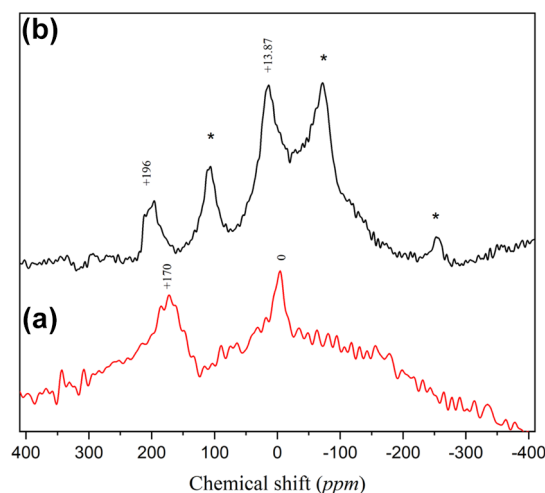


Figure 8. ^{71}Ga NMR spectra of (a) calcined Ga-MCM-22 and (b) Ga_2O_3 samples.

of trivalent gallium ions in the framework of the MWW structure.⁴⁴ Figure 2 shows the powder XRD results of the as-synthesized and calcined samples. The Ga-MCM-22 samples show that the X-ray reflection patterns complement the parent

sample. The as-synthesized Ga-MCM-22 catalyst shows the formation of layered MCM-22 (P). The calcined material showed well-behaved peaks for the MWW characteristic reflection plane in the following positions: (100) at 6.8° , (101) at 7.7° , (102) at 9.7° , (220) at 24.7° , and (310) at 25.7° . The sharp and ordered peaks imply a well-crystallized Ga-MCM-22 crystal. Broadening of the Ga-MCM-22 X-ray reflections can be due to the large Ga^{3+} species present in the framework position reducing the particle size.^{43,45}

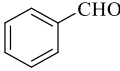
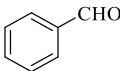
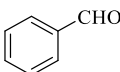
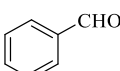
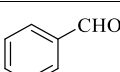
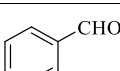
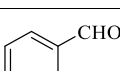
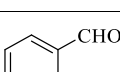
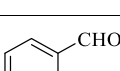
The TGA data of synthesized MCM-22 and Ga-MCM-22 are shown in Figure 3. The initial weight loss up to 180°C is due to the desorption of water species formed by the condensation of the silanol group. The Ga-MCM-22 sample showed 3% loss in this region, whereas MCM-22 showed 2.5% loss. The template removal happens between 180 and 480°C , and surface hydroxyl group condensation occurs between 480 and 650°C . The total template weight loss observed for MCM-22 was 23.5%, and Ga-MCM-22 showed a 9% total template weight loss.^{46,53} Compared to conventional MCM-22, the much lower weight loss of the present Ga-MCM-22 may be due to the larger ionic size of the trivalent gallium ion in the framework and extra-framework positions, relative to the hydrophobic environment and less template accommodation on the surface of MCM-22. The SEM images of Ga-MCM-22 show the MWW zeolite platelet morphology, arranged in a spherical shape. The Ga-MCM-22 sample shows $6.2\ \mu\text{m}$ with a flaky crystal structure (Figure 4). The SEM images support the absence of any segregated impurities,^{45,47} which agrees with the XRD studies.

Figure 5 shows the N_2 adsorption isotherm of the Ga-MCM-22 sample. The isotherm curves for the catalyst show a sharp uptake below 0.1 relative pressure (p/p_0), which are characterized by type-I isotherm, indicating the presence of a microporous structure with monolayer adsorption. The samples show the H4 type hysteresis loop generated by the narrow-slit type. Table 2 summarizes the textural properties of the samples. The BET surface area obtained for Ga-MCM-22 was $263\ \text{m}^2/\text{g}$, less than that of the conventional MCM-22. The decrease in the surface area may be due to the bulky trivalent gallium species present in the framework and extra-framework sites, which block the channel and reduce the surface area. The Ga-MCM-22 sample shows a micropore volume of $0.095\ \text{cm}^3\ \text{g}^{-1}$, suggesting that gallium ions are distributed on the framework and extra-framework sites in the MCM-22 framework, which block the pores due to their large size.^{48–50}

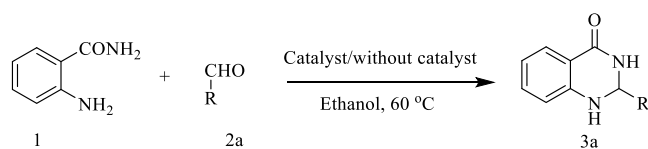
The acidic properties of the materials were investigated by employing NH_3 TPD. Figure 6 shows the corresponding results. The Ga-MCM-22 sample shows two desorption peaks in the range of 100 – 600°C . The broad peak in the lower temperature range (200 – 350°C) indicates moderate Brønsted acidity.²⁶ Desorption of ammonia causes this desorption peak from the acidic sites derived from the framework gallium species.

On the other hand, a desorption peak that appeared in a high-temperature range, corresponding to the ammonia bound to the strong acid sites (Lewis acid sites and Brønsted acidic sites),⁵¹ was produced by the trivalent gallium ions present in the extra-framework sites.³⁵ The introduction of gallium enhances the acidic strength, as evident from Figure 6. The magic angle spinning (MAS) NMR spectroscopy was conducted to explore the incorporation of gallium into the framework and extra-framework sites. The ^{29}Si and ^{71}Ga MAS

Table 3. Condensation Reaction without a Catalyst and with Different Amounts of Catalyst

Table 3. Condensation reaction without catalyst and over different amount of catalyst				
s. no.	catalyst loading	aldehyde	time (h)	yield (%)
1	no catalyst, RT		6	nil
2	no catalyst, reflux		6	15
3	5 M % Ga-MCM-22		3	55
4	10 M % Ga-MCM-22		3	90
5	15 M % Ga-MCM-22		3	95
6	20 M % Ga-MCM-22		3	95
7	gallium nitrate		6	<10
8	LiCO ₄		6	trace
9	anhy. Mg(ClO ₄) ₂		6	85%

Scheme 1. Schematic Diagram for Condensation of Anthranilamide



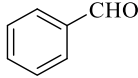
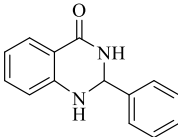
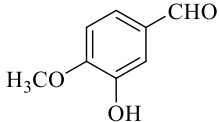
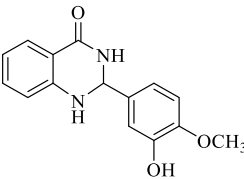
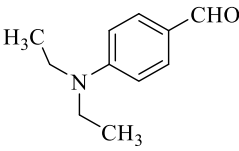
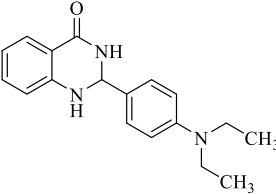
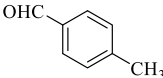
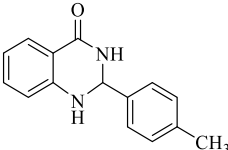
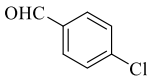
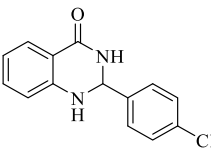
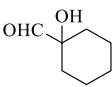
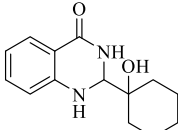
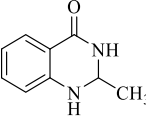
NMR spectra of the calcined Ga-MCM-22 sample are shown in Figures 7 and 8, respectively. The ²⁹Si MAS NMR spectrum shows a sharp peak at −115 ppm assigned to SiO₄ species (0 Ga) Q⁴ and a weak shoulder at −108 due to Si (1 Ga) Q³. The peaks assigned to the Q⁴ and Q³ sites observed in the spectra support the hypothesis that silicon species are present in highly crystalline environments.^{21,45,52}

The ⁷¹Ga MAS NMR spectrum of the calcined Ga-MCM-22 sample shows (Figure 8a) two peaks around +170 and 0 ppm. The peak at +170 ppm corresponds to tetrahedral Ga³⁺ species in the MCM-22 framework. The peak near 0 ppm can be due to the presence of gallium species in the octahedral environment of the extra-framework site, corresponding to

gallium oxide or gallium oxide-hydroxide species. The NMR result implies the incorporation of Ga species into the framework and the extra-framework surface of MCM-22.^{21,45,54} A comparison of the ⁷¹Ga MAS NMR spectrum of the Ga₂O₃ sample studied and the results is shown in Figure 8b. The pure Ga₂O₃ showed two doublet peaks centered around +196 and 13.8 ppm again to support the presence of gallium in fourfold and sixfold coordination sites.⁵⁴ The bands at −253 and −73 ppm correspond to side bands. There is good correlation between Ga-MCM-22 and Ga₂O₃ species.⁵⁴

Inspired by the modified acidic properties of the zeolite Ga-MCM-22 sample, we explored its catalytic activity for synthesizing 2,3-dihydroquinazolinone-4(1H)-ones. These reactions go well with the catalyst of Lewis acid. Initially, our reaction started with the addition of anthranilamide 1a and benzaldehyde 2a without any catalyst in ethanol with reflux (60 °C), and the progress of the reaction was monitored using a TLC. After 24 h, the reaction afforded 2,3-dihydroquinazolinone-4(1H)-ones in a low yield (Table 3). Then, 1a with 2a was reacted in the presence of a catalytic amount of activated Ga-MCM-22 (10 M %) in ethanol with reflux for 2 h (Scheme 1). After the successful synthesis of 2,3-dihydroquinazolinone-4(1H)-

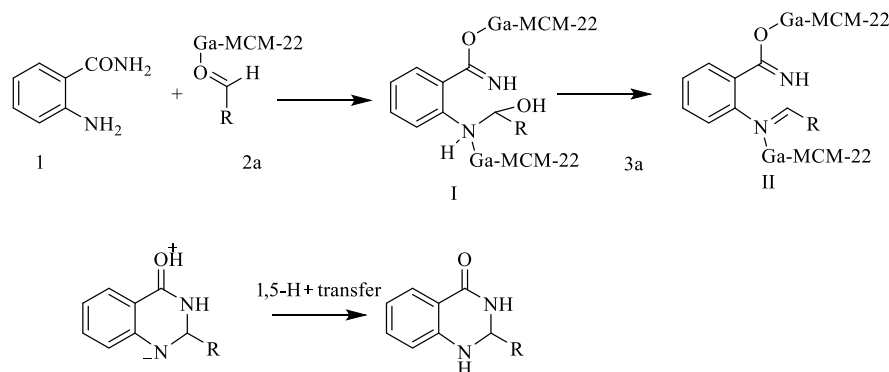
Table 4. Effects of Various Aldehydes on the Condensation of Anthranilamide Using Ga-MCM-22

Table 4. Effects of aldehydes on condensation reaction using Ga-MCM-22			
s.no.	aldehyde	product	yield
1.		 2-phenyl-2,3-dihydroquinazolin-4(1H)-one	95
2.			90
3.			85
4.			93
5.			90
6.			95
7.	$\text{OHC}-\text{CH}_3$		92

one **3a**, we explored the effect of Ga-MCM-22 at different catalytic concentrations in ethanol under reflux conditions. The outcome of this analysis is summarized in Table 3. The highest yield of 95% was achieved in the presence of 15 M % of the catalysts. A metal chloride acts by increasing the electrophilicity of the carbonyl groups. Thus, we screened the catalytic efficacy of anhydrous MgClO_4 along with gallium nitrate, gallium oxide, and Ga-MCM-22 (Table 3). The motive behind using gallium nitrate and gallium oxide is to compare the activity with the prepared catalyst. The gallium-containing MCM-22 possessing ample surface medium-strong acid sites has a high surface area. The tetrahedrally connected heteroatoms and the extra-framework cation together can

provide Lewis and Brønsted active sites, which cooperate with the in-framework protonic acid site. A drastic increase in the rate of reaction was observed in the presence of a Ga-MCM-22 catalyst using benzaldehyde **2a** and anthranilamide **1a** under reflux conditions at 60 °C, furnishing 95% of the desired product (Table 3, entry 3). It is testified that using gallosilicate as a catalyst has improved the yield of the product by enhancing electrophilicity. Gallosilicate forms an ionic bond with the carbonyl oxygen, leading to an increase in electrophilicity of the carbonyl group. Encouraged by the success, we also evaluated the optimum catalyst loading. From the results reported in Table 3 (entries 3–5), it was clear that 15 M % catalyst loading was optimal.

Scheme 2. Plausible Mechanism of Ga-MCM-22-Catalyzed Synthesis of 2,3-Dihydroquinazoline-4-(1H)-ones



Furthermore, the leaching experiment was followed by a hot filtration method to understand the catalyst's stability. The reaction mixture was filtered out, and the catalyst was separated after 30 min of reaction. Subsequently, the reaction was further proceeded with the filtrate solution, which showed negligible conversion. This supports that there is no leaching of active species under the reaction conditions. Additionally, the catalyst activity almost remains intact with more than 85% yield even after 3 cycles.

The scope of the catalyst for the condensation of anthranilamide with various cyclic, aromatic, and aliphatic aldehydes was explored in the presence of ethanol at the reflux temperature (60 °C) for 3 h. As summarized in Table 4, the condensation reaction using anthranilamide, substituted aldehydes in the presence of Ga-MCM-22, and ethanol generated six products with a percentage yield in the range of 85–95%.

The formation of the product can be explained by a plausible mechanism, as shown in Scheme 2. It seems that enhancement of the electrophilicity of the carbonyl group in the aldehyde occurred using Ga-MCM-22. An intermediate (I) was formed by the reaction of 2-anthranilamide and the activated aldehyde. Afterward, intermediate (I) was formed by the reaction of 2-aminobenzamide and the activated aldehyde. After intermediate (I) dehydration, an imine intermediate (II) was produced. However, a part of imine in this intermediate could be activated by metals. Then, intermediate (III) was prepared by an intramolecular nucleophilic attack of the amide nitrogen on the activated imine group. Then, the products were afforded by 1,5-proton transfer.

4. CONCLUSIONS

In summary, Ga-MCM-22 was prepared hydrothermally and characterized efficiently with the help of various characterization techniques. A well-crystalline MCM-22 framework was evident from powder XRD, FTIR, and SEM studies. The presence of moderate-to-strong acidic sites and a high surface area of Ga-MCM-22 were evident from sorption studies. The resultant Ga-MCM-22 proved to be a potential catalyst for the cyclocondensation of anthranilamide with various aldehydes for the synthesis of 2,3-dihydroquinazoline-4-(1H)-ones, where it showed the highest yield of 95%.

■ ASSOCIATED CONTENT

SI Supporting Information

The Supporting Information is available free of charge at <https://pubs.acs.org/doi/10.1021/acsomega.1c03704>.

¹H NMR and ¹³C NMR spectra of the synthesized compounds (PDF)

■ AUTHOR INFORMATION

Corresponding Authors

Adarsh Sahu – Department of Pharmaceutical Sciences, Dr. Harisingh Gour Central University, Sagar, Madhya Pradesh 470003, India; orcid.org/0000-0001-5190-8236; Email: adarshnipr@gmail.com

Ayyamperumal Sakthivel – Inorganic Materials & Heterogeneous Catalysis Laboratory, Department of Chemistry, School of Physical Sciences Central University of Kerala, Kasaragod, Kerala 671320, India; orcid.org/0000-0003-2330-5192; Email: Sakthiveldu@gmail.com, sakthivelcuk@cukerala.ac.in

Author

Preeti Sahu – Inorganic Materials & Heterogeneous Catalysis Laboratory, Department of Chemistry, School of Physical Sciences Central University of Kerala, Kasaragod, Kerala 671320, India

Complete contact information is available at: <https://pubs.acs.org/10.1021/acsomega.1c03704>

Notes

The authors declare no competing financial interest.

■ ACKNOWLEDGMENTS

The authors thank DST-SERB-CRG (Project No: CRG/2019/004624) for the financial grant. Mrs. P.S. is grateful to the Central University of Kerala.

■ REFERENCES

- Gallezot, P. Conversion of biomass to selected chemical products. *Chem. Soc. Rev.* **2012**, *41*, 1538–1558.
- Sakthivel, A.; Mahato, N. R.; Baskaran, T.; Christopher, J. Molybdenum carbonyl grafted onto silicate intercalated cobalt–aluminum hydrotalcite: a new potential catalyst for the hydroformylation of octene. *Catal. Commun.* **2015**, *65*, 55–61.
- Vermeiren, W.; Gilson, J. P. Impact of zeolites on the petroleum and petrochemical industry. *Top. Catal.* **2009**, *52*, 1131–1161.
- Sakthivel, A.; Iida, A.; Komura, K.; Sugi, Y.; Chary, K. V. Nanosized β -zeolites with tunable particle sizes: Synthesis by the dry gel conversion (DGC) method in the presence of surfactants, characterization and catalytic properties. *Microporous Mesoporous Mater.* **2009**, *119*, 322–330.

- (5) Yadav, R.; Sakthivel, A. Silicoaluminophosphate molecular sieves as potential catalysts for hydroisomerization of alkanes and alkenes. *Appl. Catal. A: Gen.* **2014**, *481*, 143–160.
- (6) Corma, A. From microporous to mesoporous molecular sieve materials and their use in catalysis. *Chem. Rev.* **1997**, *97*, 2373–2420.
- (7) Aleixo, R.; Elvas-Leitão, R.; Martins, F.; Carvalho, A. P.; Brigas, A.; Martins, A.; Nunes, N. Kinetic study of Friedel-Crafts acylation reactions over hierarchical MCM-22 zeolites. *Mol. Catal.* **2017**, *434*, 175–183.
- (8) Ahmad, A.; Naqvi, S. R.; Rafique, M.; Nasir, H.; Sarosh, A. Synthesis, characterization and catalytic testing of MCM-22 derived catalysts for n-hexane cracking. *Sci. Rep.* **2020**, *10*, 21786.
- (9) www.iza-online.org
- (10) Zones, S. I. Translating new materials discoveries in zeolite research to commercial manufacture. *Microporous Mesoporous Mater.* **2011**, *144*, 1–8.
- (11) Gallego, E. M.; Paris, C.; Martínez, C.; Moliner, M.; Corma, A. Nanosized MCM-22 zeolite using simple non-surfactant organic growth modifiers: synthesis and catalytic applications. *Chem. Commun.* **2018**, *54*, 9989–9992.
- (12) Corma, A.; Corell, C.; Pérez-Pariente, J. Synthesis and characterization of the MCM-22 zeolite. *Zeolites* **1995**, *15*, 2–8.
- (13) Schwanke, A. J.; Díaz, U.; Corma, A.; Pergher, S. Recyclable swelling solutions for friendly preparation of pillared MWW-type zeolites. *Microporous Mesoporous Mater.* **2017**, *253*, 91–95.
- (14) Fernandes, C. V.; Freire, V. D. A.; de Sousa, B. V. Synthesis and Characterization of MgO/MCM-22 as Catalytic Support Using the Impregnation Technique. *Mater. Sci. Forum* **2017**, *881*, 41–45.
- (15) Ostroumova, V. A.; Maksimov, A. L. MWW-Type Zeolites: MCM-22, MCM-36, MCM-49, and MCM-56. *Pet. Chem.* **2019**, *59*, 788–801.
- (16) Wu, P.; Komatsu, T.; Yashima, T. Selective formation of p-xylene with disproportionation of toluene over MCM-22 catalysts. *Microporous Mesoporous Mater.* **1998**, *22*, 343–356.
- (17) Prakash, A. M.; Wasowicz, T.; Kevan, L. Adsorbate Interactions of Paramagnetic Palladium (I) Species in Pd (II)-Exchanged Na-MCM-22 Zeolite. *J. Phys. Chem. B* **1997**, *101*, 1985–1993.
- (18) du, H.; Olson, D. H. J. Surface Acidic Properties of A HMCM-22 Zeolite: Collidine Poisoning and Hydrocarbon Adsorption Studies. *J. Phys. Chem. B* **2002**, *106*, 395–400.
- (19) Kumar, N.; Lindfors, L. E. Synthesis, characterization and application of H-MCM-22, Ga-MCM-22 and Zn-MCM-22 zeolite catalysts in the aromatization of n-butane. *Appl. Catal. A-Gen.* **1996**, *147*, 175–187.
- (20) Safont, A. C.; Cabello, C. P.; Areán, C. O.; Palomino, G. T. Brønsted acidity of H-[Ga]-ZSM-5 zeolites as determined by variable-temperature IR spectroscopy. *Catal. Today* **2020**, *345*, 71–79.
- (21) Choudhary, V. R.; Kinage, A. K.; Sivadinarayana, C.; Devadas, P.; Sansare, S. D.; Guisnet, M. H-Gallosilicate (MFI) Propane Aromatization Catalyst: Influence of Si/Ga Ratio on Acidity, Activity and Deactivation Due to Coking. *J. Catal.* **1996**, *158*, 34–50.
- (22) Choudhary, V. R.; Sivadinarayana, C.; Kinage, A. K.; Devadas, P.; Guisnet, M. H-Gallosilicate (MFI) propane aromatization catalyst Influence of calcination temperature on acidity, activity and deactivation due to coking. *Appl. Catal. A-Gen.* **1996**, *136*, 125–142.
- (23) Kim, S. J.; Jung, K. D.; Joo, O. S. Synthesis and Characterization of Gallosilicate Molecular Sieve with the MCM-22 Framework Topology. *J. Porous Mater.* **2004**, *11*, 211–218.
- (24) Wang, J.; Zhang, F.; Hua, W.; Yue, Y.; Gao, Z. Dehydrogenation of propane over MWW-type zeolites supported gallium oxide. *Catal. Commun.* **2012**, *18*, 63–67.
- (25) Zheng, B.; Hua, W.; Yue, Y.; Gao, Z. Dehydrogenation of Propane to Propene over Different Polymorphs of Gallium Oxide. *J. Catal.* **2005**, *232*, 143–151.
- (26) Chu, C. T. W.; Chang, C. D. Isomorphous substitution in zeolite frameworks. 1. Acidity of surface hydroxyls in [B]-, [Fe]-, [Ga]-, and [Al]-ZSM-5. *J. Phys. Chem.* **1985**, *89*, 1569–1571.
- (27) Fechete, I.; Dumitriu, E.; Caulet, P.; Lutic, D.; Kessler, H. Synthesis and physicochemical characterisation of (Si, Ga)-Mcm-22 Zeolite. Toluene disproportionation reaction. *Stud. Cercet. Stiint.: Chim. Ing. Chim., Biotechnol. Ind. Aliment.* **2007**, *8*, 355–368.
- (28) Morrison, R. A.; Rubin, M. K. Gallium-containing zeolite MCM-22. U.S. Patent 5,284,643A, February 8, 1994.
- (29) Morrison, R. A.; Rubin, M. K. Gallium-containing zeolite MCM-22. U.S. Patent 5,382,742, January 17, 1995.
- (30) Fricke, R.; Kosslick, H.; Lischke, G.; Richter, M. Incorporation of gallium into zeolites: syntheses, properties and catalytic application. *Chem. Rev.* **2000**, *100*, 2303–2406.
- (31) Long, Q. S.; Liu, L. W.; Zhao, Y. L.; Wang, P. Y.; Chen, B.; Li, Z.; Yang, S. Fabrication of furan-functionalized quinazoline hybrids: their antibacterial evaluation, quantitative proteomics, and induced phytopathogen morphological variation studies. *J. Agric. Food Chem.* **2019**, *67*, 11005–11017.
- (32) Mishra, S.; Das, D.; Sahu, A.; Verma, E.; Patil, S.; Agarwal, R. K.; Gajbhiye, A. Electronegativity in Substituted-4(H)-quinazolinones Causes Anxiolysis without a Sedative-hypnotic Adverse Reaction in Female Wistar Rats. *Cent. Nerv. Syst. Agents Med. Chem.* **2020**, *20*, 26–40.
- (33) Mishra, S.; Das, D.; Sahu, A.; Patil, S.; Agarwal, R. K.; Gajbhiye, A. Transition Metal-free Approach for the Synthesis of 2-substituted Quinazolin-4(3H)-one via Anhydrous Magnesium Perchlorate. *Curr. Organocatal.* **2020**, *7*, 118–123.
- (34) Sahu, A.; Kumar, D.; Agrawal, R. K. Antileishmanial Drug Discovery: Synthetic Methods, Chemical Characteristics, and Biological Potential of Quinazolines and its Derivatives. *Antiinflamm. Antiallergy Agents Med. Chem.* **2017**, *16*, 3–32.
- (35) Marzaro, G.; Guiotto, A.; Chilin, A. Quinazoline derivatives as potential anticancer agents: a patent review. *Expert Opin. Ther. Pat.* **2012**, *22*, 223–252.
- (36) Aly, A. A. Synthesis of Novel Quinazoline Derivatives as Antimicrobial Agents. *Chin. J. Chem.* **2003**, *21*, 339–346.
- (37) Malasala, S.; Ahmad, M. N.; Akunuri, R.; Shukla, M.; Kaul, G.; Dasgupta, A.; Madhavi, Y. V.; Chopra, S.; Nanduri, S. Synthesis and evaluation of new quinazoline-benzimidazole hybrids as potent antimicrobial agents against multidrug resistant *Staphylococcus aureus* and *Mycobacterium tuberculosis*. *Eur. J. Med. Chem.* **2021**, *212*, No. 112996.
- (38) Sahu, A.; Mishra, S.; Sahu, P.; Gajbhiye, A.; Agrawal, R. K. Indium (III) Chloride: An Efficient Catalyst for One-Pot Multi-component Synthesis of 2, 3-dihydroquinazolin-4 (1H)-ones. *Curr. Organocatal.* **2018**, *5*, 137–144.
- (39) Abdollahi-Alibeik, M.; Shabani, E. Synthesis of 2, 3-dihydroquinazolin-4 (1H)-ones catalyzed by zirconium (IV) chloride as a mild and efficient catalyst. *Chin. Chem. Lett.* **2011**, *22*, 1163–1166.
- (40) Larksarp, C.; Alper, H. Palladium-catalyzed cyclocarbonylation of o-iodoanilines with heterocumulenes: regioselective preparation of 4(3H)-quinazolinone derivatives. *J. Org. Chem.* **2000**, *65*, 2773–2777.
- (41) Jasra, R. V.; Das, J.; Unnikrishnan, A.; Sakthivel, A. A method for the preparation of MWW type zeolite. U.S. Patent 9,359,216, June 7, 2016.
- (42) Sahu, P.; Eniyarppu, S.; Ahmed, M.; Sharma, D.; Sakthivel, A. Cerium ion-exchanged layered MCM-22: preparation, characterization and its application for esterification of fatty acids. *J. Porous Mater.* **2018**, *25*, 999–1005.
- (43) Ravishankar, R.; Bhattacharya, D.; Jacob, N. E.; Sivasanker, S. Characterization and catalytic properties of zeolite MCM-22. *Microporous Mater.* **1995**, *4*, 83–93.
- (44) Sahu, P.; HariPriya, T. V.; Sreenavya, A.; Shanbhag, G. V.; Augustin, A.; Sakthivel, A. Alkali/alkaline earth ion-exchanged and palladium dispersed MCM-22 zeolite as a potential catalyst for eugenol isomerization and Heck coupling reactions. *J. Chem. Sci.* **2020**, *132*, 153–161.
- (45) Ma, X.; Zhou, D.; Chu, X.; Li, D.; Wang, J.; Song, W.; Xia, Q. Highly selective isomerization of biomass β -pinene over hierarchically acidic MCM-22 catalyst. *Microporous Mesoporous Mater.* **2017**, *237*, 180–188.

(46) Roth, W. J.; Gil, B.; Makowski, W.; Slawek, A.; Korzeniowska, A.; Grzybek, J.; Siwek, M.; Michorczyk, P. Framework-substituted cerium MCM-22 zeolite and its interlayer expanded derivative MWW-IEZ. *Catal. Sci. Technol.* **2016**, *6*, 2742–2753.

(47) Sahu, P.; Ganesh, V.; Sakthivel, A. Oxidation of a lignin-derived-model compound: Iso-eugenol to vanillin over cerium containing MCM-22. *Catal. Commun.* **2020**, *145*, No. 106099.

(48) Baskaran, T.; Joshi, A.; Kamalakar, G.; Sakthivel, A. A solvent free method for preparation of β -amino alcohols by ring opening of epoxides with amines using MCM-22 as a catalyst. *Appl. Catal. A: Gen.* **2016**, *524*, 50–55.

(49) Hu, J.; Wu, S.; Li, Z.; Peng, L.; Fu, X.; Wang, X.; Guan, J.; Kan, Q. Nano-MoO₃-modified MCM-22 for methane dehydroaromatization. *Appl. Organometal. Chem.* **2015**, *29*, 638–645.

(50) Hazm, J. E.; Caullet, P.; Paillaud, J. L.; Soulard, M.; Delmotte, L. *Microporous Mesoporous Mater.* **2001**, *43*, 11–25.

(51) Sakthivel, A.; Baskaran, T. Amino-Silane Functionalized MCM-22 Zeolite and Its Application on Nitroaldol Condensation. *Adv. Porous Mater.* **2016**, *4*, 206–211.

(52) Nakai, M.; Miyake, K.; Inoue, R.; Ono, K.; al Jabri, H.; Hirota, Y.; Uchida, Y.; Tanaka, S.; Miyamoto, M.; Oumi, Y.; Kong, C. Y.; Nishiyama, N. Dehydrogenation of propane over high silica *BEA type gallosilicate (Ga-Beta). *Catal. Sci. Technol.* **2019**, *9*, 6234–6239.

(53) Sahu, P.; Tincy, A.; Sreenavya, A.; Shanbhag, G.; Sakthivel, A. Molybdenum Carbonyl Grafted on Amine-Functionalized MCM-22 as Potential Catalyst for Iso-Eugenol Oxidation. *Catal. Lett.* **2021**, *151*, 1336–1349.

(54) Massiot, D.; Farnan, I.; Gautier, N.; Trumeau, D.; Trokiner, A.; Coutures, J. P. ⁷¹Ga and ⁶⁹Ga nuclear magnetic resonance study of β -Ga₂O₃: resolution of four- and six-fold coordinated Ga sites in static conditions. *Solid State Nucl. Magn. Reson.* **1995**, *4*, 241–248.